

Electronic Supplementary Information

Scalability of Voltage-Controlled Filamentary and Nanometallic Resistance Memories

*Yang Lu[‡], Jong Ho Lee[‡], and I-Wei Chen**

[‡]These authors contribute equally to this work.

Department of Materials Science and Engineering, University of Pennsylvania,
Philadelphia, PA 19104-6272, USA

E-mail: iweichen@seas.upenn.edu

Table S1. Summary of V_{on}^* , V_{off}^* , and $|V^*|$ extracted by different methods for two types of devices of various sizes under various switching/sweeping conditions.

System	Size (μm^2)	Method	$ V^* $ (V)	V_{off}^* (V)	V_{on}^* (V)
Filamentary HfO _x	7.25 ~ 100	Linear fitting w/o I_{cc} (Fig. 2b). $ V^* $ from fitting both on- and off- data, $V_{on/off}^*$ from fitting on-/off-data only	0.99	-0.95	1.00
	7.25	Load-sharing of V_{app} w/o I_{cc} (Fig. 2c, 4c). $ V^* $ from averaging all $ V_{on}^* $ and $ V_{off}^* $	0.98	-0.96	0.99
	25			-0.95	1.00
	100			-0.95	1.00
$10^3 \sim 10^5$	Direct reading of V_{app} w/ I_{cc} (Fig. 4c). $ V^* $ from averaging all $ V_{on}^* $ and $ V_{off}^* $	1.05	-0.90	1.20	
Nanomteallic SiN _{4/3} :Pt	7.25 ~ 100	Linear fitting w/o I_{cc} (Fig. 2b). $ V^* $ from fitting both on- and off- data, $V_{on/off}^*$ from fitting on-/off-data only	0.97	-1.00	0.97
	7.25	Load-sharing of V_{app} w/o I_{cc} (Fig. 2d, 4d). $ V^* $ from averaging all $ V_{on}^* $ and $ V_{off}^* $	0.97	-0.98	0.96
	25			-0.99	0.94
	100			-0.98	0.97
$0.1 \sim 10^5$	Direct reading of V_{app} w/ I_{cc} (Fig. 4d). $ V^* $ from averaging all $ V_{on}^* $ and $ V_{off}^* $	0.99	-1.00	0.98	

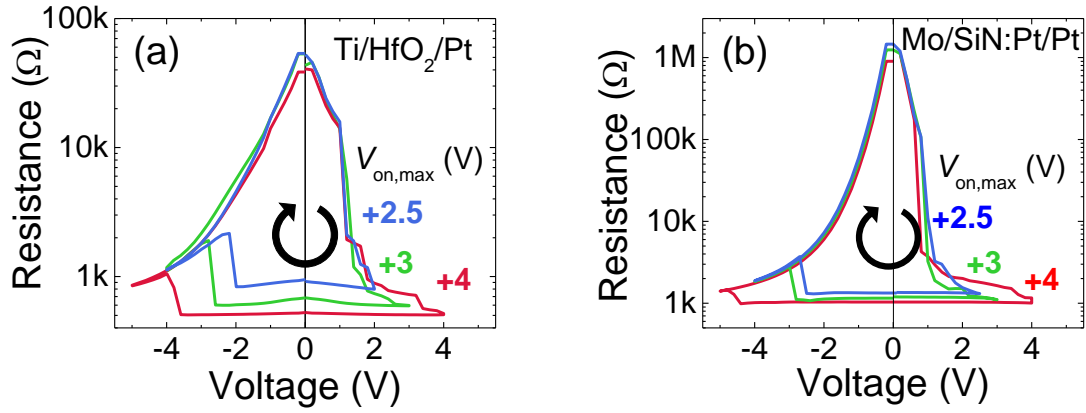


Figure S1. Same-cell R - V switching curves with different maximum \pm sweep voltage ($V_{\text{on,max}}$ indicated for positive polarity) for (a) Ti/HfO₂/Pt RRAM, and (b) Mo/SiN_{4/3}:Pt/Pt RRAM. Cell radius: 80 μm . In both cases, a larger current during the on-switching positive sweep leads to a progressive decrease of LRS and increase of off-switching voltage. R_{LRS} approaches an asymptote ($R_{\text{S}}+R_{\text{load}}$). On-switching always occurs around a critical voltage V^* of +1 V, as further verified in Fig. 2b.

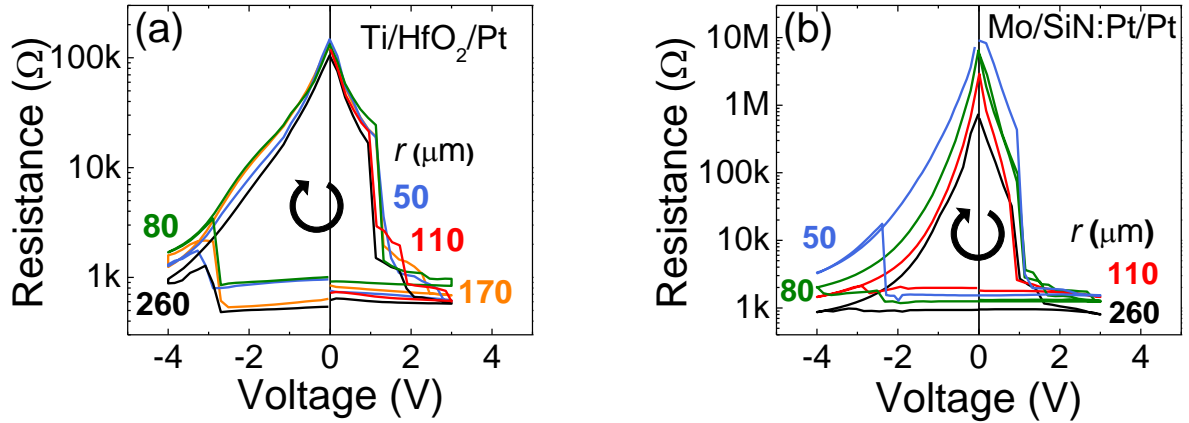


Figure S2. Area scaling of resistance switching in Ti/HfO₂/Pt RRAM and Mo/SiN_{4/3}:Pt/Pt RRAM. *R-V* switching curves of different device radius *r* of (a) Pt/HfO₂/Ti RRAM and (b) Mo/SiN_{4/3}:9.3%Pt/Pt RRAM. On-switching occurs at a size-independent critical voltage *V*^{*} of +1 V in both RRAMs. Size-independent HRS and LRS resistance of Ti/HfO₂/Pt, and size-independent LRS but size-dependent HRS of Mo/SiN_{4/3}:Pt/Pt, are summarized in Fig. 2g-h.

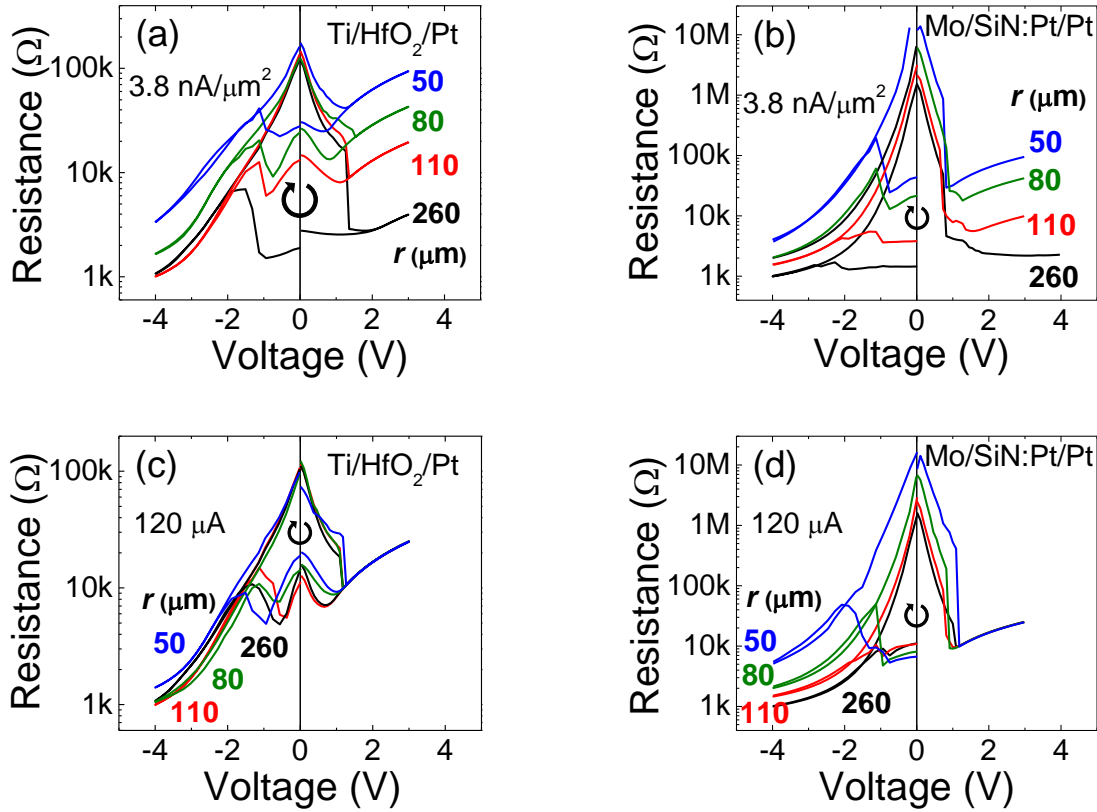


Figure S3. R - V curves of different device radius r under compliance control. (a) Ti/HfO₂/Pt RRAM and (b) Mo/Si₃N₄:9.3%Pt/Pt RRAM, with same constant current density 3.8 nA/μm² set for on-switching, resulting in area-dependent LRS in both. (c) Ti/HfO₂/Pt RRAM (d) Mo/Si₃N₄:9.3%Pt/Pt RRAM, with same constant current 120 μA set for on-switching, resulting in area-independent LRS in both. Under both sets of compliance, zero-voltage HRS is area-dependent in Mo/Si₃N₄:9.3%Pt/Pt (b, d), but area-independent in Ti/HfO₂/Pt (a, c).

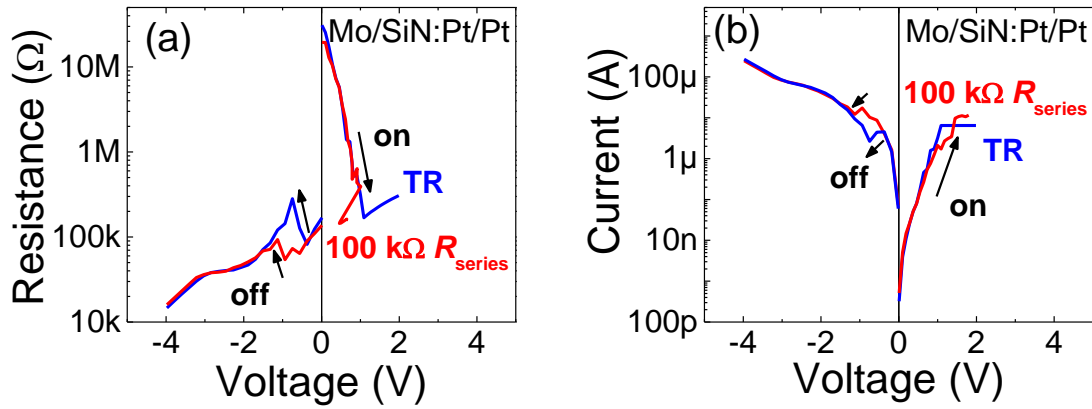


Figure S4. Comparison of switching curves of Mo/Si₃N₄:9.3%Pt/Pt RRAM in two configurations of compliance control, with a transistor (TR), and with a 100 kΩ resistor (R_{series}). (a) Resistance vs. voltage on the RRAM device. (b) Current vs. voltage applied to the RRAM device. Arrows indicate on- and off-switching. Voltage sharing on R_{series} causes a higher off-switching voltage in both (a) and (b).

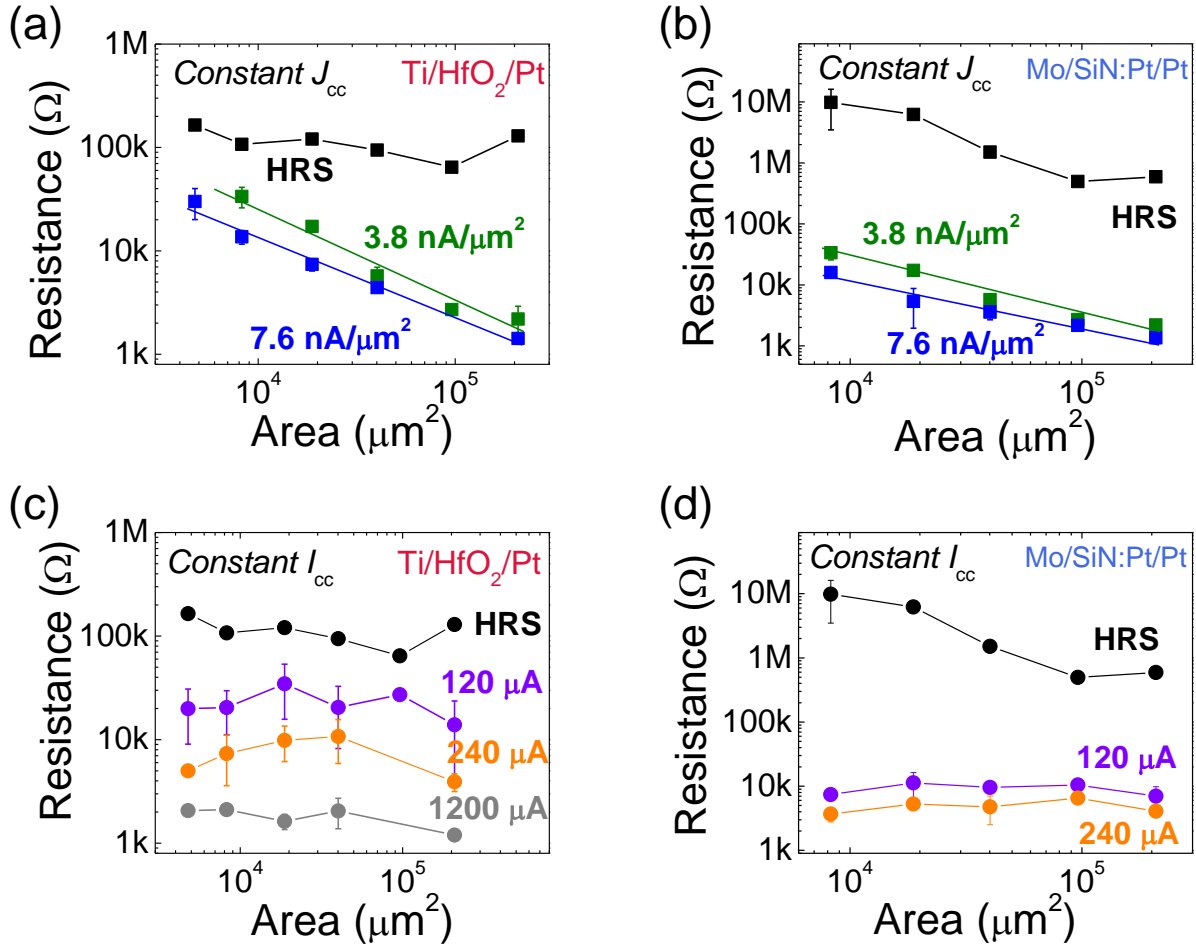


Figure S5. Resistance scaling of Ti/HfO₂/Pt RRAM and Mo/SiN_{4/3}:Pt/Pt RRAM under current compliance. (a) and (c): Ti/HfO₂/Pt device with area-independent HRS has area-dependent LRS under the same current density (a), but area-independent LRS under the same current (c). (b) and (d): Mo/SiN_{4/3}:9.3%Pt/Pt device with area-dependent HRS has area-dependent LRS under the same current density (b), but area-independent LRS under the same current (d). Error bars are from average of 10 tests. Current and current density control in 1T1R configuration. Straight lines next to LRS data in (a) and (b): predicted $R_{LRS} = V^*/Aj_{cc}$ similar to the one in Fig. 4f.

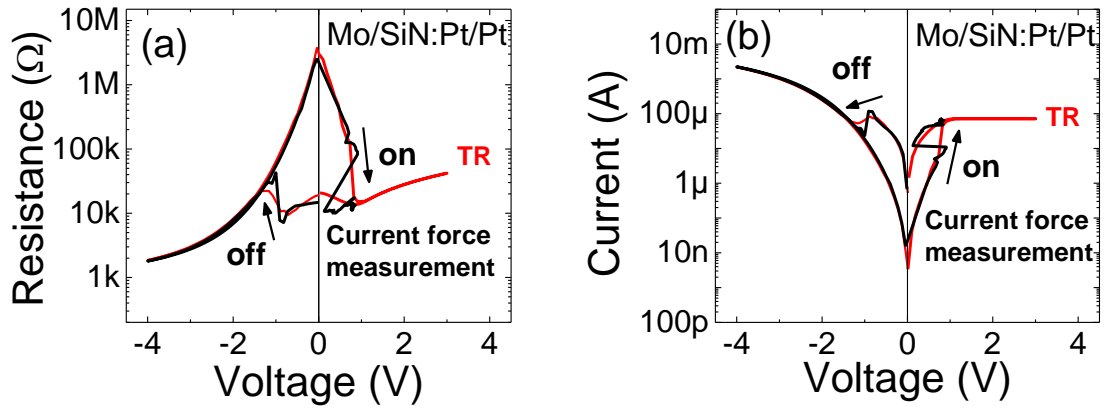


Figure S6. Comparison of switching curves of Mo/SiN_{4/3}:9.3%Pt/Pt RRAM in voltage sweep with compliance provided by transistor (TR, red), and in current (force) sweep, with current ramping from 0 to 70 μA under a positive bias causing on-switching (black curves under negative bias). The red curves under negative bias for off-switching were obtained in voltage sweep without transistor. (a) Resistance vs. voltage curves and (b) current vs. voltage curves. Arrows indicate switching directions. In current sweep, a constant onset voltage around 1 V triggers on-switching that results in a voltage drop as well as a resistance drop.

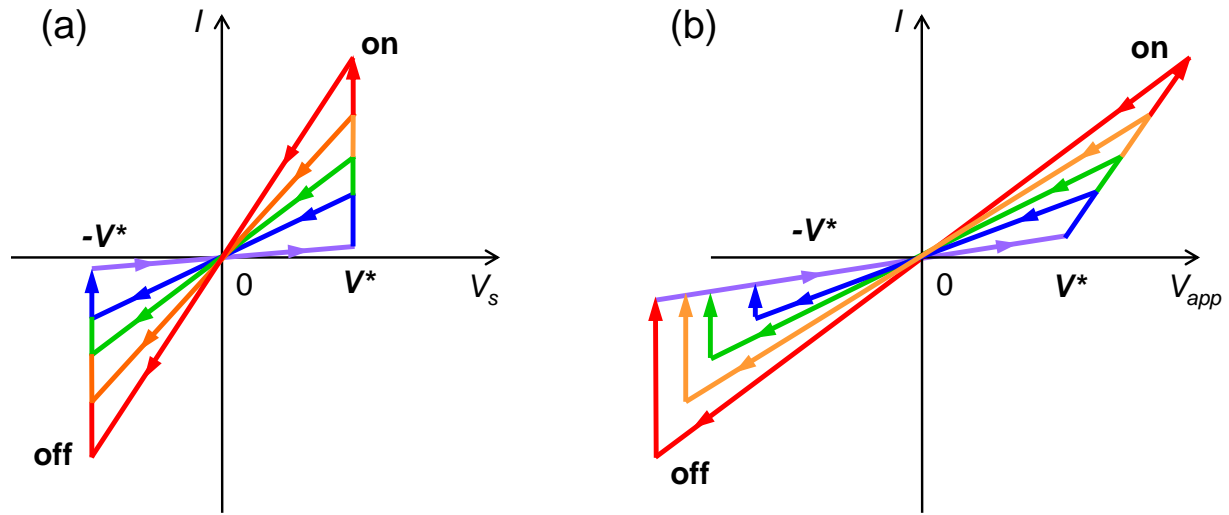


Figure S7. Schematic I - V curves of voltage-controlled bipolar resistance switching. (a) Current (I) vs voltage on R_s (V_s): On- and off-switching occur at $V_s = \pm V^*$ to reach certain current I . (b) Current (I) vs total applied voltage V_{app} . Unlike (a), on- and off-switching occur at various voltages because of load sharing, but maximum V_{app} is the same in both polarity. As V_{app} increases during on-switching, I - V curve of switched LRS asymptotically approaches $I = V_{app}/R_{load}$. Arrows indicate sweeping directions. Refer to equivalent circuit in Fig. 2a.

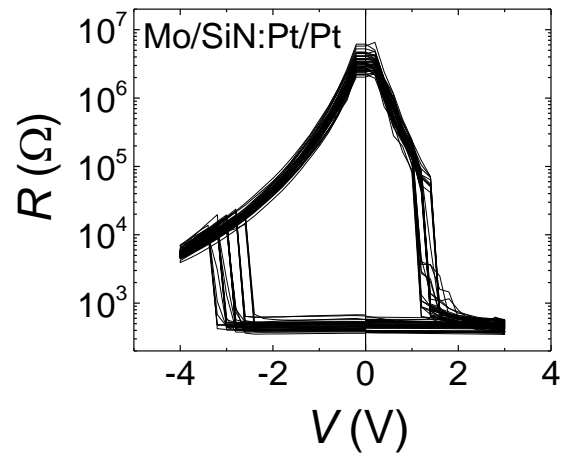


Figure S8. Overlapping of 100 cycling R - V switching curves of Mo/SiN_{4/3}:Pt/Pt device with radius of 2.5 μm show good cycle-to-cycle uniformity of switching characteristics.